Loss of the Mismatch Repair Protein MSH6 in Human Glioblastomas Is Associated with Tumor Progression during Temozolomide Treatment

Daniel P. Cahill,[1,2] Kymberly K. Levine,[1] Rebecca A. Betensky,[5] Patrick J. Codd,[2] Candice A. Romany,[1] Linsey B. Reavie,[1] Tracy T. Batchelor,[3] P. Andrew Futreal,[6] Michael R. Stratton,[6] William T. Curry,[2,3] A. John Iafrate,[1] and David N. Louis[1,4]

Abstract

Purpose: Glioblastomas are treated by surgical resection followed by radiotherapy [X-ray therapy (XRT)] and the alkylating chemotherapeutic agent temozolomide. Recently, inactivating mutations in the mismatch repair gene *MSH6* were identified in two glioblastomas recurrent post-temozolomide. Because mismatch repair pathway inactivation is a known mediator of alkylator resistance *in vitro*, these findings suggested that *MSH6* inactivation was causally linked to these two recurrences. However, the extent of involvement of *MSH6* in glioblastoma is unknown. We sought to determine the overall frequency and clinical relevance of *MSH6* alterations in glioblastomas.

Experimental Design: The *MSH6* gene was sequenced in 54 glioblastomas. MSH6 and O^6-methylguanine methyltransferase (MGMT) immunohistochemistry was systematically scored in a panel of 46 clinically well-characterized glioblastomas, and the corresponding patient response to treatment evaluated.

Results: *MSH6* mutation was not observed in any pretreatment glioblastoma (0 of 40), whereas 3 of 14 recurrent cases had somatic mutations ($P = 0.015$). MSH6 protein expression was detected in all pretreatment (17 of 17) cases examined but, notably, expression was lost in 7 of 17 (41%) recurrences from matched post – XRT + temozolomide cases ($P = 0.016$). Loss of MSH6 was not associated with O^6-methylguanine methyltransferase status. Measurements of *in vivo* tumor growth using three-dimensional reconstructed magnetic resonance imaging showed that MSH6-negative glioblastomas had a markedly increased rate of growth while under temozolomide treatment (3.17 versus 0.04 cc/mo for MSH6-positive tumors; $P = 0.020$).

Conclusions: Loss of MSH6 occurs in a subset of post – XRT + temozolomide glioblastoma recurrences and is associated with tumor progression during temozolomide treatment, mirroring the alkylator resistance conferred by *MSH6* inactivation *in vitro*. MSH6 deficiency may therefore contribute to the emergence of recurrent glioblastomas during temozolomide treatment.

Authors' Affiliations: [1]Molecular Pathology Unit, [2]Neurosurgical Service, [3]Brain Tumor Center, and [4]Center for Cancer Research, Massachusetts General Hospital and Harvard Medical School; [5]Department of Biostatistics, Harvard School of Public Health, Boston, Massachusetts; and [6]Cancer Genome Project, Wellcome Trust Sanger Institute, Hinxton, United Kingdom

Received 8/29/06; revised 12/8/06; accepted 12/27/06.

Grant support: Institute of Cancer Research, the Wellcome Trust, Brain Tumor Society Seth Harris Feldman Research Award, National Brain Tumor Foundation GBM grant, American Brain Tumor Association Fellowship, American Association of Neurosurgeons NREF Fellowship, and the NIH.

The costs of publication of this article were defrayed in part by the payment of page charges. This article must therefore be hereby marked *advertisement* in accordance with 18 U.S.C. Section 1734 solely to indicate this fact.

Note: Supplementary data for this article are available at Clinical Cancer Research Online (http://clincancerres.aacrjournals.org/).

Requests for reprints: David N. Louis, Pathology Service, Massachusetts General Hospital, 55 Fruit Street, Warren 2, Boston, MA 02114. Phone: 617-726-5690; Fax: 617-726-5684; E-mail: dlouis@partners.org.

©2007 American Association for Cancer Research.

doi:10.1158/1078-0432.CCR-06-2149

Cancers evolve during tumor progression by the clonal selection of genetic alterations in tumor cells. Successive waves of clonal outgrowth overcome a multitude of selection barriers during neoplastic development. In addition, cancers face further selection pressures once they are diagnosed and treatment is initiated, and they continue to accumulate genetic alterations that confer selective growth advantage by allowing escape from the tumoricidal effects of treatment. In this regard, glioblastomas, the most frequent primary human brain tumor, are a prototypical human neoplasia: they accumulate mutations in oncogenes (e.g., *EGFR*) and tumor suppressor genes (e.g., *PTEN*; ref. 1), display clinical responsiveness to X-ray therapy (XRT) and the alkylating chemotherapeutic agent temozolomide (2), but ultimately fail these therapies and progress to fatal outcomes.

In a recent large-scale sequence analysis of malignant gliomas, somatic truncating mutations in the mismatch repair

Downloaded from clincancerres.aacrjournals.org on September 30, 2020. © 2007 American Association for Cancer Research.

gene *MSH6* were identified in two recurrent human glioblastomas (3). Both tumors had large numbers of somatic mutations within a mutational signature consistent with alkylator treatment, and both had been treated with temozolomide. Prior studies in murine embryonic stem cells (4), Chinese hamster cell lines (5), human lymphoblastoid cells (6–8), and human cancer cells (9, 10) have shown that *MSH6* inactivation confers tolerant cell growth under cytotoxic doses of alkylating agents *in vitro*. Importantly, tolerant cells can be subsequently resensitized to alkylating agents by reintroduction of wild-type *MSH6* (9, 10), establishing the direct role of the *MSH6* gene in mediating this chemoresistance effect (11). We therefore hypothesized that *MSH6* inactivation in tumor subclones may have contributed to their clonal expansion during temozolomide treatment and emergence as clinical recurrences in these two cases.

However, the overall frequency of *MSH6* alterations in glioblastomas is unknown. Previous reports have identified homozygous germ line mutations of *MSH6* in isolated cases of syndromic children with brain tumors (12, 13), but heterozygous germ line or somatic mutations of *MSH6* have not been reported in typical adult patients with sporadic glioblastoma. Moreover, clinical phenotypic surveys of large *MSH6* kindreds with familial colorectal or endometrial cancer have not identified an increased risk of glioblastoma in patients with heterozygous germ line *MSH6* mutations (14, 15). Nonetheless, because heterozygous germ line mutations in the canonical mismatch repair genes *MSH2* and *MLH1* can cause the mixed colonic-and-glial tumor spectrum of Turcot syndrome (16), it is possible that yet undiscovered germ line or somatic *MSH6* mutations could contribute to the development of a subset of glioblastomas.

In addition, this initial finding of *MSH6* mutations in two tumors is counterbalanced by a substantial body of evidence that temozolomide responsiveness in glioblastomas can be predicted before treatment by determining the O^6-methylguanine methyltransferase (MGMT) status (17, 18). MGMT is a well-characterized enzyme that catalyzes removal of the methyl-conjugate from O^6-methylguanine, one of the nucleotide modifications that results from temozolomide treatment. High levels of MGMT activity are thought to offset alkylator modification of tumor DNA, thereby limiting temozolomide antitumor activity. Levels of MGMT have been assessed by promoter methylation analysis (17), direct enzymatic assay (18), or immunohistochemistry (19), and elevated levels correspond to more rapid tumor progression. Further complicating the understanding of these two pathways, it seems that both can be operant in the development of alkylator resistance *in vitro* (20), with mismatch repair deficiency serving as an alternative escape route when cancer cells have low levels of MGMT expression (21). It is thus possible that both pathways could contribute to clinical recurrences in glioblastoma patients receiving temozolomide.

We therefore sought to determine the frequency of *MSH6* mutation or loss of protein expression in glioblastomas. In addition, we examined the relationship between MSH6 loss, adjuvant treatment modality, and MGMT status, and characterized the clinical consequences of MSH6 loss. To this end, we analyzed the mutational status and expression of *MSH6* in both pretreatment and posttreatment glioblastoma samples, compared this pattern with the MGMT expression status of these samples, and examined the radiologic and clinical treatment course of the cohort in detail.

Materials and Methods

Tumor and DNA stocks. Tumors and peripheral blood lymphocytes for normal controls were banked under Institutional Review Board–approved protocols at the Massachusetts General Hospital. Tumor DNA was extracted from tumor specimens or early cell-culture passage after histologic confirmation (PureGene kit, Gentra Systems, Minneapolis, MN). Tumor and normal DNA for sample xT5165 and treatment information were kindly provided by Drs. Gregory Riggins and Charles Eberhart (The Johns Hopkins Hospital, Baltimore, MD). The tumors assembled for sequencing analysis were identified based on two criteria: histologically confirmed glioblastoma (WHO grade IV) and availability of appropriate quality specimen (i.e., fresh-frozen surgical resection or early cell-culture passage) for DNA sequence–based analyses.

For the panel of tumors assembled for immunohistochemical analyses, three criteria were used to identify patients: histologically confirmed glioblastoma (WHO grade IV); treatment with a chemotherapeutic regimen that included temozolomide; and availability of appropriate formalin-fixed, paraffin-embedded specimen. Five samples were analyzed by both sequencing and immunohistochemistry (three with wild-type *MSH6*, two with mutant *MSH6*). As can be seen in Tables 1 and 2, their results were concordant across both assessment modalities. As a control for adjuvant treatment modality, an additional eight glioblastomas from XRT-only–treated cases were also studied.

PCR amplification and sequencing. PCR primers were derived from ref. 14, covering >98% of the *MSH6* coding sequence (sequences available on request). Amplification was done using Taq-Platinum DNA polymerase (Invitrogen, Carlsbad, CA). One primer from each pair was tagged with M13F universal sequencing primer to facilitate subsequent fluorescent dye-terminator sequencing (Agencourt Biosciences, Beverly, MA). Of a total of 752 reactions, 705 were successfully amplified and sequenced, for a sequence coverage rate of >93%.

Immunohistochemistry. Monoclonal antibodies to MSH6/GTBP (clone 44, BD Biosciences, San Jose, CA) and MGMT (MT3.1, Chemicon, Temecula, CA) were used for immunohistochemistry on formalin-fixed, paraffin-embedded sections. Antigen retrieval was achieved with 20-min (MSH6) or 15-min (MGMT) incubation in 10 mmol/L sodium citrate buffer at pH 6.0. Overnight 4°C incubations with a 1:100 (MSH6) or 1:50 (MGMT) dilution were done (Vectastatin Elite avidin-biotin complex kit, Vector Laboratories, Burlingame, CA). Positive control tissue consisted of nuclear staining in colonic crypt cells and the germinal centers of lymph nodes (MSH6) or cytoplasmic and nuclear stating in colon cancer and normal brain (MGMT). Scoring was done in a blinded fashion by two reviewers (D.P.C. and D.N.L.).

Tumor growth measurements. Magnetic resonance imaging (MRI) volume calculations were done on axial imaging sections through the tumor mass using the Vitrea2 3D volumetric software (Vital Images, Inc., Minnetonka, MI). Personnel scoring tumor volume were blinded to the molecular stratification of the tumors. Tumor volume was assessed using standard criteria of T1-post-gadolinium sequence enhancing volume, correcting for acute surgical residua by exclusion of pre-gadolinium T1 sequence enhancement. Tumor growth rate was calculated on matched pairs by determining the T1-enhancing volume from the MRI obtained at the initiation of alkylator therapy (which was typically the postoperative MRI following surgical biopsy or debulking resection), and subtracting it from the T1-enhancing tumor volume on the MRI obtained immediately before cessation of alkylator therapy. This change in volume was then divided by the difference in time between the two studies to calculate an overall growth rate during alkylator therapy. Similar calculations were done for FLAIR sequences, which assess the magnitude of tumor-associated edema.

In one recurrence (corresponding to tumor specimen xT4899), a second MRI study was not obtained before cessation of therapy;

Downloaded from clincancerres.aacrjournals.org on September 30, 2020. © 2007 American Association for Cancer Research.

Table 1. Sequence analysis of *MSH6* in glioblastomas

Sample ID	Treatment	Sample	MSH6 mutation
xT3017	XRT + TMZ	Posttreatment	Het C1453T, Q485X; Het G3907A, A1303T
xT3162	XRT + TMZ, IV BCNU, thioguanine	Posttreatment	Hom delG2425, V809X
xT5165	Unknown treatment	Posttreatment	Het A560C, K187T; Het T794G, F265C
xT104	XRT + TMZ, oncolytic virus, implantable BCNU wafer	Posttreatment	Wild-type
xT2993	XRT + TMZ, IV BCNU, implantable BCNU wafer	Posttreatment	Wild-type
xT3072	Unspecified "chemotherapy," XRT	Posttreatment	Wild-type
xT3296	XRT + TMZ, radio-iodine125 EGFR mAb	Posttreatment	Wild-type
xT3378	XRT + TMZ, IV BCNU, radio-iodine125 EGFR mAb	Posttreatment	Wild-type
xT3768	XRT + TMZ	Posttreatment	Wild-type
xT155	XRT	Posttreatment	Wild-type
xT177	XRT + CPT11	Posttreatment	Wild-type
xT601	XRT	Posttreatment	Wild-type
xT1178	XRT + PCV	Posttreatment	Wild-type
xT1201	Procarbazine	Posttreatment	Wild-type
40 cases	—	Pretreatment	Wild-type

NOTE: The top-listed samples (*shaded*) are derived from patients that had received treatment with temozolomide or unspecified chemotherapy. Details of treatment and mutation status are as noted. Sample ID list for the 40 pretreatment cases available on request. *MSH6* status of samples xT155, xT924, xT2560, xT3017, xT3058, and xT3162 has previously been reported in ref. 3.
Abbreviations: TMZ, temozolomide; BCNU, 1,3-bis(2-chloroethyl)-1-nitrosourea; EGFR, epidermal growth factor receptor; PCV, procarbazine/1-(2-chloroethyl)-3-cyclohexyl-L-nitrosourea/vincristine.

therefore, we used data calculated from an MRI scan that occurred 16 days after the last dose of temozolomide because it was still within the standard treatment window of 28 days for a single cycle of temozolomide therapy. One patient (corresponding to tumor specimen xT3162) was excluded from tumor growth analyses because the follow-up MRI sequences available were obtained more than 4 months after cessation of temozolomide therapy; this patient's tumor growth data are appended to Supplementary Table S1 and can be seen as essentially comparable to the other cases, but were censored because of the length of time outside of alkylating therapy without radiologic assessment.

Statistical analysis. Pretreatment cases were defined as a patient's first surgical resection, and recurrences as the first surgical resection after failure of the specified treatment modality (XRT or XRT + temozolomide). Two-sided, 0.05 level Fisher's exact tests were used to compare two independent proportions. An exact binomial confidence interval was calculated for the frequency of negative MSH6 expression at recurrence following temozolomide treatment. An exact, two-sided, 0.05 level McNemar's test was used to compare the frequency of MSH6-negative expression at recurrence following temozolomide treatment with that in the pretreatment sample. To adjust for the length bias induced by the sampling of recurrent cases, semiparametric truncation-adjusted Kaplan-Meier estimates (22), parametric Weibull estimates, and log-rank tests were used for the analyses of age at diagnosis (right truncated by age at recurrence), length of alkylator treatment (right truncated by time from diagnosis to recurrence), time to recurrence (right truncated by time to death or end of follow-up), and time from diagnosis to death (left truncated by time to recurrence). Exact, two-sided, 0.025 level (Bonferroni adjusted) Wilcoxon tests were used to evaluate for differences in tumor growth rates under treatment, as measured by T1 post-gadolinium enhancement and FLAIR hyperintensity. For the expression of growth rate per month, the growth rate per day was multiplied by 30 days.

Results

Sequence analysis of MSH6. Our prior sequencing study analyzed six glioblastomas for *MSH6* alterations and found somatic mutations in two tumors. To survey the overall spectrum of *MSH6* mutation in glioblastoma, we analyzed the *MSH6* coding sequence in an additional 48 glioblastomas. Thirty-seven were pretreatment tumors whereas 11 were recurrent tumors. These samples were not preselected based on their treatment regimen, and therefore the recurrences had previously received a range of alkylator, nonalkylator, or even no chemotherapy. The clinical details of these samples and sequence analysis results are listed in Table 1. No mutations of *MSH6* were identified in the pretreatment tumors. Therefore, germ line or somatic *MSH6* mutations do not seem to contribute significantly to the pretreatment development of glioblastoma. In the recurrent samples, one tumor (xT5165) had two sequence alterations that resulted in predicted amino acid substitutions. One was an A-to-C transversion at nucleotide 560 leading to a lysine-to-threonine substitution at amino acid position 187. The other was a T-to-G transversion at nucleotide 794 resulting in a phenylalanine-to-cysteine replacement at amino acid position 265. Neither of the alterations was found in the patient's normal DNA.

Combining data from these 48 tumors with our prior findings yielded a total of 3 *MSH6*-mutant cases among 14 recurrent tumors, whereas none of the 40 pretreatment tumors had mutations. Because the recurrence rate of glioblastoma is nearly 100%, random sampling of recurrences is unlikely to introduce significant selection bias with respect to prior pretreatment status. With this in mind, comparison of the frequency of mutation in our pretreatment and posttreatment samples suggests that *MSH6* mutation is associated with recurrence ($P = 0.015$).

Immunohistochemistry for MSH6 expression. These results, in light of the known selectivity of the mismatch repair pathway in mediating alkylator resistance *in vitro*, raised the possibility that selection for *MSH6* inactivation could be a treatment-specific phenomenon. Moreover, the treatment regimens varied among these patients, possibly accounting for the minority of recurrent cases with detectable *MSH6* mutations. We therefore sought to evaluate *MSH6* in a second sample set focused on glioblastomas that had undergone adjuvant treatment with the standard-of-care alkylating agent temozolomide. To maximize

Downloaded from clincancerres.aacrjournals.org on September 30, 2020. © 2007 American Association for Cancer Research.

the assessable yield of MSH6 status, we pursued immunohistochemistry of formalin-fixed, paraffin-embedded specimens, which constitute the majority of clinically well-annotated material in glioblastoma trial settings. Most glioblastoma biopsy specimens are not sufficient to afford genomic amplification and large-scale sequence analyses; fortunately, there is extensive experience validating the usefulness of immunohistochemistry to detect *MSH6* inactivation in hereditary colon and endometrial cancer (14, 15, 23, 24).

We scored both MSH6 and MGMT status in a total of 46 glioblastomas (Table 2). Within this group, 38 specimens were from 21 patients who had received treatment with XRT + temozolomide. Because our study design necessitated selection of patients who had undergone two surgeries, we examined the baseline demographic characteristics of those patients treated with XRT + temozolomide to assess for selection bias. The patient cohort was 71% male, with median age at diagnosis of 53 years. These data are indicative of a patient group similar to those reported in the recent large prospective study of XRT + temozolomide (2). Of the tumors studied, 34 were matched pairs derived from 17 patients' pre– and post–XRT + temozolomide surgical resections, providing the additional benefit of certainty about the pretreatment MSH6 status.

In the matched pretreatment specimens, every tumor examined (17 of 17) stained positively for MSH6 expression. The staining displayed variability, ranging from <10% to >50% of the total tumor cell mass in any given case. However, even accounting for this variability, every pretreatment glioblastoma evaluated was unequivocally positive for MSH6 expression (Table 2), whereas normal brain sections do not stain for MSH6 expression (Fig. 1). Thus, there seems to be an induction of MSH6 protein expression in pretreatment glioblastomas, consistent with previous immunohistochemistry studies of MSH6 in other tumors types (14, 15, 23, 24) and of other mismatch repair genes in glioblastoma (25).

In matched post–XRT + temozolomide tumors from the same patients, a range of MSH6 staining was also observed, with four cases showing an increase in staining and four cases showing stable intensity. Strikingly, however, staining for MSH6 was completely absent in seven of these cases (Fig. 1). This loss of MSH6 expression at recurrence within the matched pairs was significantly different from that at diagnosis ($P = 0.016$, based on the seven tumor pairs with discordant pretreatment and posttreatment expression). Furthermore, in four additional post–XRT + temozolomide tumors, three had absence of MSH6 protein. Therefore, in total, 10 of 21 post–XRT + temozolomide recurrent tumors displayed absence of MSH6 by immunohistochemical analysis.

To isolate the effect of temozolomide chemotherapy comparatively, we analyzed an additional eight recurrent tumors

Table 2. MSH6 and MGMT immunohistochemical analysis

Treatment modality	Pre- and post-treatment sample ID	Pretreatment MGMT	Post–XRT + temozolomide MGMT	Pretreatment MSH6	Post–XRT + temozolomide MSH6
XRT + temozolomide	xT4981/xT5089	–	–	+	++
	xT3546/xT4717	+	+	++	++
	xT4142/xT3692	–	–	+++	++
	xT3559/xT4328	–	–	+++	++
	xT2989/xT3296	–	–	++	++
	xT4107/xT3648	+	+	++	+++
	xT4106/xT3307	–	–	+++	+++
	xT3506/xT3768	+	+	++	+++
	xT4170/xT4987	–	–	+	++
	xT4213/xT4869	+	+	+	+
	xT4901/xT4899	+	+	++	–
	xT4991/xT3017	+	+	+	–
	xT3495/xT4161	+	+	++	–
	xT3893/xT4870	n/s	+	+	–
	xT3513/xT4718	–	–	+	–
	xT4136/xT4900	+	+	+++	–
	xT4838/xT5065	+	+	+++	–
XRT + temozolomide	—/xT104		+		++
	—/xT5046		n/s		–
	—/xT4803		–		–
	—/xT3162		–		–
XRT-only	—/xT4986		–		++
	—/xT4903		–		++
	—/xT4977		–		++
	—/xT4975		+		++
	—/xT2422		+		++
	—/xT2703		–		++
	—/xT3303		+		++
	—/xT4985		+		++

NOTE: MSH6 and MGMT status in matched samples from 17 patients' pre– and post–XRT + temozolomide surgical resections. Additionally listed are four post–XRT + temozolomide and eight post–XRT-only samples where the pretreatment sample was unavailable for study. MSH6 scored with a system of –, nil or scant staining; +, <10% of cells stained positive in the nucleus; ++, 10% to 50%; and +++, >50% positive. MGMT scored using +, >20% positive staining; –, <20% staining.
Abbreviation: n/s, assay not successfully done.

Downloaded from clincancerres.aacrjournals.org on September 30, 2020. © 2007 American Association for Cancer Research.

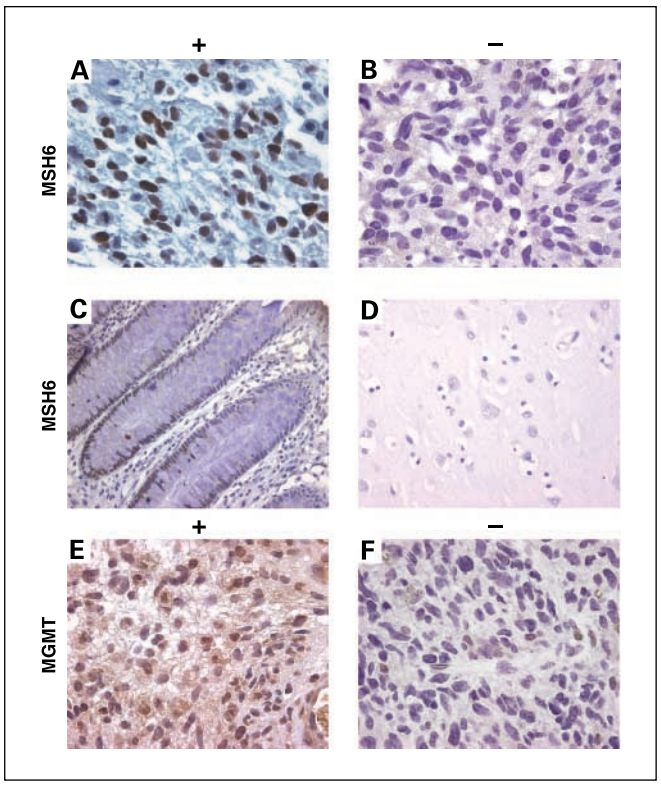

Fig. 1. MSH6 and MGMT immunohistochemistry. Immunohistochemistry was done with monoclonal antibodies specific for MSH6 (*A*, sample xT3307; *B*, xT3162), with controls of normal colonic epithelium (*C*) and normal brain (*D*). The larger field of view for (*C*) shows MSH6 expression in the crypt and transit-amplifying cells, but not in differentiated colonic epithelium. *E* and *F,* MGMT immunohistochemistry (*E*, sample xT3506; *F*, xT4142).

from patients who had received adjuvant treatment solely with XRT. These samples served as a treatment-modality control group; because current clinical practice does not allow withholding radiation treatment from eligible patients, it was not possible to assemble a cohort of patients who had solely received temozolomide in the absence of XRT. These post–XRT-only specimens were all positive for MSH6 expression (8 of 8 tumors). Comparing these recurrences to post–XRT + temozolomide recurrences as independent samples based on treatment modality (with the presumption of no significant selection bias among the recurrences with respect to their pretreatment status), there was a significant difference with respect to the frequency of MSH6 expression loss at recurrence between post–XRT + temozolomide and post–XRT-only glioblastomas ($P = 0.012$), providing evidence that MSH6 loss is specifically associated with the temozolomide alkylator component of combined adjuvant therapy.

MGMT. As noted above, decreased MGMT expression is a predictor of improved glioblastoma prognosis. It is therefore possible that acquisition of increased MGMT expression itself contributes to the emergence of resistant clones during temozolomide treatment. Given the association of MGMT status with treatment response, it is also possible that MSH6 status at recurrence is linked to pretreatment MGMT status. To determine the relationship between MGMT status, MSH6 status, and post–XRT + temozolomide recurrence, we assessed MGMT immunohistochemistry within our panel of tumors.

MGMT staining was successfully analyzed in 44 of the 46 samples, including 16 of 17 pretreatment tumors. We found a range of MGMT staining similar to prior estimates of the frequency of MGMT absence (17–19), with 7 of 16 staining negatively for MGMT and 9 of 16 scoring moderately or strongly positive (Fig. 1; Table 2). Similarly consistent with prior immunohistochemistry analyses (19), absence of MGMT in the pretreatment tumor displayed a trend toward prolonged overall survival ($P = 0.151$). To evaluate changes in MGMT status during adjuvant therapy, we analyzed MGMT expression in the available matched post–XRT + temozolomide specimens. For any individual patient, pretreatment MGMT status was maintained in the post–XRT + temozolomide sample, including all seven glioblastomas that were MGMT negative before temozolomide treatment (Table 2). These data suggest that the induction of MGMT expression that can be seen in model systems of alkylator exposure (20) may not be frequent under the treatment dosing of temozolomide in current clinical practice. Also, we did not find a significant association between

Table 3. Baseline characteristics of clinical and radiologic measures

	MSH6-positive ($n = 11$), median (range)	MSH6-negative ($n = 9$), median (range)	*P*
Age at recurrence, y	49 (23-70)	56 (31-67)	NS
Gender (% male)	64	78	
Calculated pretreatment tumor volume, cc	11.79 (1.65-46.59)	5.12 (0-53.73)	NS
Pretreatment T1-post-gadolinium enhancement volume, cc	12.6 (1.8-54.85)	9.75 (0-53.73)	NS
Pretreatment T1 enhancement volume (i.e., pre-gadolinium), cc	1.37 (0-41.06)	0 (0-11.33)	NS
Pretreatment FLAIR volume, cc	43.16 (5-178.4)	52.75 (8.29-229.6)	NS
Recurrence T1-post-gadolinium enhancement volume, cc	9.15 (5.2-44.1)	16.17 (4.19-82.83)	NS
Recurrence FLAIR volume, cc	56.13 (8.05-185.3)	57.53 (10.92-353.2)	NS
Time elapsed between initial and recurrence scans, d	170 (71-364)	153 (57-432)	NS
Rate of FLAIR change, cc/d	0.009 (−0.645-0.406)	0.060 (−0.221-1.258)	NS
Rate of T1-post-gadolinium enhancement change, cc/d	0.001 (−0.087-0.068)	0.106 (−0.055-0.288)	0.020

NOTE: Radiologic assessment factors were compared between the two groups of patients with glioblastoma recurrences determined by MSH6-positive or MSH6-negative immunohistochemical staining. No significant differences were noted between potential confounding measures. Tumor growth rate, as assessed by rate of T1-post-gadolinium enhancement change, was higher in the MSH6-negative group.
Abbreviation: NS, not significant ($P > 0.025$).

Downloaded from clincancerres.aacrjournals.org on September 30, 2020. © 2007 American Association for Cancer Research.

MGMT pretreatment status and MSH6 posttreatment status ($P = 0.145$), although our analyses suggest a possible correlative trend that might be further uncovered in larger studies.

Clinical correlation. To characterize the clinical features of patients whose tumors displayed MSH6 loss, clinical data were analyzed from patients treated with XRT + temozolomide. Medical records were abstracted for the dates of initial surgery, length of treatment with temozolomide and other alkylating agents, dates of recurrent surgery, and date of death. Comparing the two independent groups determined by MSH6-positive ($n = 11$) and MSH6-negative ($n = 10$) scoring at recurrence, we noted no significant differences in possible confounding factors such as age at diagnosis, time to initiation of alkylator treatment, length of alkylator treatment, or time to recurrent surgery ($P = 0.998$, $P = 0.523$, $P = 0.820$, and $P = 0.698$, respectively).

To determine the treatment consequences of MSH6 loss, we used MRI for *in vivo* calculations of tumor growth rates during temozolomide treatment in patients stratified for MSH6 status. For all patients analyzed by immunohistochemistry above, we identified matched pairs of MRI scans, one corresponding to the initiation of alkylating chemotherapy inclusive of temozolomide and one immediately before cessation of this treatment; appropriate matched pairs were identified for 20 of 21 patients. In aggregate, MRI data were assessed spanning 3,879 days across a total alkylator treatment time of 4,496 days, covering >85% of the clinical treatment window. To exclude the possibility of systematic confounding biases arising during the clinical care and radiologic assessment of these patients, we examined several aspects of the timing and clinical conditions of the patients' treatment assignments and MRI schedules. We found no significant differences between MSH6-positive and MSH6-negative tumors with respect to either the time between the start of alkylator treatment and the initial MRI or the time between cessation of alkylator treatment and the final assessment MRI. Furthermore, to exclude the possibility that tumors were being assessed at different stages of progression due to clinical factors, we examined radiologic proxy measures of clinical performance such as the volume of tumor, as assessed by T1-gadolinium-enhancing signal, or the volume of edema, as assessed by FLAIR signal, and found no significant differences between the two groups when comparing either the pretreatment or posttreatment scans (Table 3, with the full clinical-radiologic data set available in Supplementary Table S1).

We then calculated *in vivo* tumor growth rates under temozolomide treatment by comparing the volume of tumor on the initial scan to the volume present at cessation of temozolomide treatment. Interestingly, we could not detect a correlation between pretreatment MGMT status and the rate of tumor growth under temozolomide treatment. Importantly however, MSH6-negative glioblastomas showed a markedly increased rate of growth while being treated with temozolomide, with a median T1-gadolinium enhancing signal change of +3.17 cc/mo (0.106 cc/d), whereas median MSH6-positive tumor growth was only +0.04 cc/mo (0.001 cc/d) under temozolomide treatment (Table 3; Fig. 2). The magnitude of this difference was in accordance with *in vitro* studies of *MSH6* function in alkylator-tolerant growth and was significant ($P = 0.020$). With the caveat that there may be subtle confounding factors in these comparisons that we were unable to detect due to our cohort size, this increased growth rate

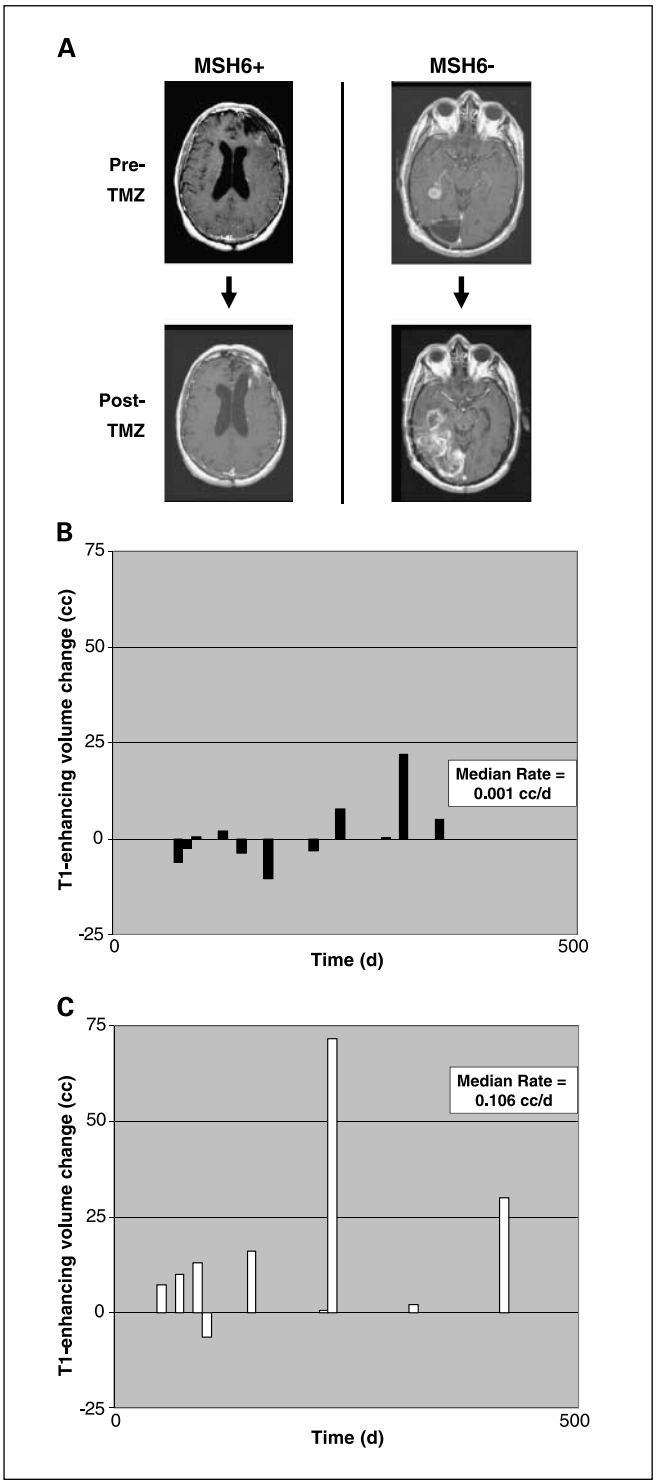

Fig. 2. Three-dimensional MRI tumor growth calculations. *A,* representative post-gadolinium enhancement T1 sequence axial sections through the tumor mass, corresponding to the initiation of alkylating chemotherapy inclusive of temozolomide and immediately before cessation of this treatment. Left, MSH6-positive case showing recurrent tumor sample xT3692; 254 d elapsed between initial and final scan. Right, MSH6-negative case showing recurrent glioblastoma sample xT4161; 249 d elapsed between initial and final scan. Multiple axial imaging sections through the tumor mass were summated to determine enhancing tumor volume. *B,* for 11 MSH6-positive tumors, volume change versus time elapsed between initial and follow-up MRI scan. The median rate of volume change was 0.001 cc/d. *C,* for nine MSH6-negative tumors, volume change versus time, with a median rate of 0.106 cc/d. Full clinical/radiologic data set available in Supplementary Table S1.

Downloaded from clincancerres.aacrjournals.org on September 30, 2020. © 2007 American Association for Cancer Research.

suggests that MSH6 loss *in vivo* corresponds to decreased clinical responsiveness to temozolomide and subsequent recurrent tumor growth during treatment, mirroring the alkylator resistance conferred by *MSH6* inactivation *in vitro*.

Discussion

Our findings show that loss of MSH6 expression occurs in a significant subset of post–XRT + temozolomide recurrent glioblastomas and is associated with the progressive growth of these tumors while they are under temozolomide treatment. These findings parallel *in vitro* studies documenting the frequent emergence of mismatch repair deficiency in cell line subclones after selection and outgrowth in alkylating agents (26, 27). Importantly, whereas many factors have been proposed to mediate therapeutic resistance based on studies of cancer cells exposed to differing doses of chemotherapeutic agents *in vitro*, our observations were made on patients receiving the clinical standard-of-care doses of an oral alkylating agent, indicating that MSH6 loss seems to recapitulate its known *in vitro* alkylator resistance role in glioblastoma patients *in vivo*.

This extension of *in vitro* mechanistic studies to an *in vivo* system has significant implications regarding patient-drug interactions; for example, it can be reasonably surmised that drug delivery across the blood-brain barrier and tumor vasculature is not a rate-limiting factor in temozolomide treatment failure in cases with MSH6 loss because the recurrent tumor cell mass displays the hallmarks of a selection pressure mediated by direct exposure to the drug itself. Likewise, *in vitro* studies indicate that there is an interactive specificity between drug and pathway in the development of resistance: mismatch repair pathway defects can mediate up to a 100-fold resistance to alkylating agents but only show ~2-fold resistance to the intrastrand cross-linking agent cisplatin and no significant resistance to agents such as topoisomerase inhibitors or interstrand cross-linkers such as mitomycin C or 1-(2-chloroethyl)-3-cyclohexyl-L-nitrosourea (28). Our *in vivo* tumor growth rate measurements reflect a similar degree of difference in clinical progression between MSH6-negative and MSH6-positive glioblastomas during temozolomide treatment. However, the prediction from *in vitro* studies would be that chemotherapeutic agents with different mechanisms (29, 30) may still prove effective in MSH6-negative glioblastomas because the cellular resistance associated with MSH6 absence is specific for exposure to alkylators.

Previous reports have indicated that alkylator resistance can be mediated either by MGMT overexpression or mismatch repair deficiency (20, 21, 25, 31). Importantly, our analyses of recurrent glioblastoma samples indicate that MSH6 loss occurred independently of the MGMT status of the pretreatment tumor, indicating that MSH6 loss is not merely a proxy of MGMT status. Our data illustrate the relationship between these two mechanisms in patients who have undergone temozolomide treatment, indicating that whereas pretreatment tumor MGMT levels may be linked to primary resistance, acquisition of further increased expression does not seem to be a common cause of emergent temozolomide resistance in the clinical setting. Interestingly, many current salvage chemotherapeutic regimens propose increasing the dosing schedule of temozolomide, in variations known collectively as "dose-dense" modifications (32), in an attempt to overcome increased levels of MGMT activity. However, it seems that MSH6 loss can occur during temozolomide treatment regardless of MGMT status, with subsequent clonal outgrowth leading to recurrence through an alternative route of treatment escape. Dose-dense modifications may therefore prove ineffective for patients with MSH6-negative tumors because the window of therapeutic index available for this substantially myelotoxic therapy may have closed.

Given that there may be several operative mechanisms for functional *MSH6* alteration, our immunohistochemistry results may underestimate the contribution of altered *MSH6* pathway function to temozolomide insensitivity. Our sequencing efforts show clear evidence of somatic mutational alteration and clonal selection in some recurrent tumors. However, at the protein level, the MSH6 protein participates in a large multiprotein complex with other mismatch repair proteins to coordinate mismatch binding, mismatch repair, and DNA damage checkpoint signaling. Recent work has shown that O^6-methylguanine-thymine mismatches are specifically bound by the heterodimeric MSH2:MSH6 MutSα complex to drive activation of the ATR/Chk1 S-G_2 phase checkpoint pathway (33). Posttranslational changes in the subcellular localization of the MSH2:MSH6 complex occurs in response to genotoxic agents (34), communicating repair activity signals to checkpoint machinery (35). This checkpoint signaling pathway is thought to mediate much of the tumoricidal effect of alkylating chemotherapy (11). Because study of mismatch repair checkpoint pathway signaling remains an active area of investigation, it is likely that other novel candidates for analysis in treatment-tolerant tumors will emerge.

Indeed, the existence of post–XRT + temozolomide glioblastomas that retain or even increase MSH6 expression highlights the probability that alternative genetic mechanisms do contribute to temozolomide evasion. Whereas it is plausible that alterations in other mismatch repair genes such as *MSH2* or *MLH1* could play a similar role to *MSH6* in glioblastoma, the canonical microsatellite instability typical of *MSH2* or *MLH1* deficiency is rarely found in adult sporadic pretreatment or posttreatment glioblastoma specimens (36, 37). Notably, as opposed to other mismatch repair genes, *MSH6* deficiency is not associated with high levels of microsatellite instability (11). Furthermore, *MSH6*, but not other mismatch repair genes, is preferentially targeted *in vitro* in unbiased chemotherapy resistance genetic screens (4). With this in mind, we speculate that temozolomide may engender a selection pressure specifically targeting for MSH6 loss instead of other mismatch repair genes, as tumor subclones negotiate a balance between the increased mutation load of mismatch repair deficiency and the selective growth advantage of temozolomide insensitivity.

Given the variability among salvage therapies within recurrent glioblastoma patient cohorts, further analyses in a more uniformly treated group of patients will be needed to confirm our findings and provide further insight into such gene-specific and treatment-specific hypotheses. Current clinical practice withholds surgical intervention in many cases of recurrence due to a perceived lack of benefit relative to the risk of surgery in rapidly declining patients. With the advent of combined XRT + temozolomide treatment, more glioblastoma patients are likely to undergo recurrent surgical intervention, affording important opportunities for well-controlled molecular

Downloaded from clincancerres.aacrjournals.org on September 30, 2020. © 2007 American Association for Cancer Research.

pathologic studies of chemotherapeutic response and escape pathways. By better understanding the molecular basis for treatment evasion and subsequent clinical failure, we can envision the rational design of targeted combination therapeutic strategies that will limit the emergence of such treatment escape in future patients.

Acknowledgments

We thank the patients who participated in this research through donation of blood and tumor samples; the Massachusetts General Hospital Neuroradiology 3D Lab for use of 3D volumetric software; and Drs. Gregory Riggins and Charles Eberhart for providing tumor and normal DNA samples.

References

1. Louis DN. Molecular pathology of malignant gliomas. Annu Rev Pathol Mech Dis 2006;1:97–117.
2. Stupp R, Mason WP, van den Bent MJ, et al. Radiotherapy plus concomitant and adjuvant temozolomide for glioblastoma. N Engl J Med 2005;352:987–96.
3. Hunter C, Smith R, Cahill DP, et al. A hypermutation phenotype and somatic MSH6 mutations in recurrent human malignant gliomas after alkylator chemotherapy. Cancer Res 2006;66:3987–91.
4. Guo G, Wang W, Bradley A. Mismatch repair genes identified using genetic screens in Blm-deficient embryonic stem cells. Nature 2004;429:891–5.
5. Hickman MJ, Samson LD. Role of DNA mismatch repair and p53 in signaling induction of apoptosis by alkylating agents. Proc Natl Acad Sci U S A 1999;96:10764–9.
6. Kat A, Thilly WG, Fang WH, Longley MJ, Li GM, Modrich P. An alkylation-tolerant, mutator human cell line is deficient in strand-specific mismatch repair. Proc Natl Acad Sci U S A 1993;90:6424–8.
7. Tomita-Mitchell A, Kat AG, Marcelino LA, Li-Sucholeiki XC, Goodluck-Griffith J, Thilly WG. Mismatch repair deficient human cells: spontaneous and MNNG-induced mutational spectra in the HPRT gene. Mutat Res 2000;450:125–38.
8. Szadkowski M, Iaccarino I, Heinimann K, Marra G, Jiricny J. Characterization of the mismatch repair defect in the human lymphoblastold MT1 cells. Cancer Res 2005;65:4525–9.
9. Umar A, Koi M, Risinger JI, et al. Correction of hypermutability, *N*-methyl-*N*′-nitro-*N*-nitrosoguanidine resistance, and defective DNA mismatch repair by introducing chromosome 2 into human tumor cells with mutations in MSH2 and MSH6. Cancer Res 1997;57:3949–55.
10. Lettieri T, Marra G, Aquilina G, et al. Effect of hMSH6 cDNA expression on the phenotype of mismatch repair-deficient colon cancer cell line HCT15. Carcinogenesis 1999;20:373–82.
11. Jiricny J. The multifaceted mismatch-repair system. Nat Rev Mol Cell Biol 2006;7:335–46.
12. Hegde MR, Chong B, Blazo ME, et al. A homozygous mutation in MSH6 causes Turcot syndrome. Clin Cancer Res 2005;11:4689–93.
13. Menko FH, Kaspers GL, Meijer GA, Claes K, van Hagen JM, Gille JJ. A homozygous MSH6 mutation in a child with cafe-au-lait spots, oligodendroglioma and rectal cancer. Fam Cancer 2004;3:123–7.
14. Buttin BM, Powell MA, Mutch DG, et al. Penetrance and expressivity of MSH6 germline mutations in seven kindreds not ascertained by family history. Am J Hum Genet 2004;74:1262–9.
15. Berends MJ, Wu Y, Sijmons RH, et al. Molecular and clinical characteristics of MSH6 variants: an analysis of 25 index carriers of a germline variant. Am J Hum Genet 2002;70:26–37.
16. Hamilton SR, Liu B, Parsons RE, et al. The molecular basis of Turcots syndrome. N Engl J Med 1995;332:839–47.
17. Hegi ME, Diserens A, Gorlia T, et al. MGMT gene silencing and benefit from temozolomide in glioblastoma. N Engl J Med 2005;352:997–1003.
18. Silber JR, Blank A, Bobola MS, Ghatan S, Kolstoe DD, Berger MS. O^6-Methylguanine-DNA methyltransferase-deficient phenotype in human gliomas: frequency and time to tumor progression after alkylating agent-based chemotherapy. Clin Cancer Res 1999;5:807–14.
19. Nakasu S, Fukami T, Baba K, Matsuda M. Immunohistochemical study for O^6-methylguanine-DNA methyltransferase in the non-neoplastic and neoplastic components of gliomas. J Neurooncol 2004;70:333–40.
20. Bearzatto A, Szadkowski M, Macpherson P, Jiricny J, Karran P. Epigenetic regulation of the MGMT and hMSH6 DNA repair genes in cells resistant to methylating agents. Cancer Res 2000;60:3262–70.
21. Liu LL, Markowitz S, Gerson SL. Mismatch repair mutations override alkyltransferase in conferring resistance to temozolomide but not to 1,3-bis(2-chloroethyl) nitrosourea. Cancer Res 1996;56:5375–9.
22. Wang M-C. A semiparametric model for randomly truncated data. J Am Stat Assoc 1989;84:742–8.
23. Barnetson RA, Tenesa A, Farrington SM, et al. Identification and survival of carriers of mutations in DNA mismatch-repair genes in colon cancer. N Engl J Med 2006;354:2751–63.
24. Hampel H, Frankel WL, Martin E, et al. Screening for the Lynch syndrome (hereditary nonpolyposis colorectal cancer). N Engl J Med 2005;352:1851–60.
25. Friedman HS, McLendon RE, Kerby T, et al. DNA mismatch repair and *O*-6-alkylguanine-DNA alkyltransferase analysis and response to temodal in newly diagnosed malignant glioma. J Clin Oncol 1998;16:3851–7.
26. Branch P, Aquilina G, Bignami M, Karran P. Defective mismatch binding and a mutator phenotype in cells tolerant to DNA Damage. Nature 1993;362:652–4.
27. Bardelli A, Cahill DP, Lederer G, et al. Carcinogen-specific induction of genetic instability. Proc Natl Acad Sci U S A 2001;98:5770–5.
28. Papouli E, Cejka P, Jiricny J. Dependence of the cytotoxicity of DNA-damaging agents on the mismatch repair status of human cells. Cancer Res 2004;64:3391–4.
29. Liu L, Taverna P, Whitacre CM, Chatterjee S, Gerson SL. Pharmacologic disruption of base excision repair sensitizes mismatch repair-deficient and -proficient colon cancer cells to methylating agents. Clin Cancer Res 1999;5:2908–17.
30. Trivedi RN, Almeida KH, Fornsaglio JL, Schamus S, Sobol RW. The role of base excision repair in the sensitivity and resistance to temozolomide-mediated cell death. Cancer Res 2005;65:6394–400.
31. Pepponi R, Marra G, Fuggetta MP, et al. The effect of O^6-alkylguanine-DNA alkyltransferase and mismatch repair activities on the sensitivity of human melanoma cells to temozolomide, 1,3-bis(2-chloroethyl)1-nitrosourea, and cisplatin. J Pharmacol Exp Ther 2003;304:661–8.
32. Vera K, Djafari L, Faivre S, et al. Dose-dense regimen of temozolomide given every other week in patients with primary central nervous system tumors. Ann Oncol 2004;15:161–71.
33. Yoshioka K, Yoshioka Y, Hsieh P. ATR kinase activation mediated by MutSα and MutLα in response to cytotoxic *O*(6)-methylguanine adducts. Mol Cell 2006;22:501–10.
34. Christmann M, Tomicic MT, Kaina B. Phosphorylation of mismatch repair proteins MSH2 and MSH6 affecting MutSα mismatch-binding activity. Nucleic Acids Res 2002;30:1959–66.
35. Hawn MT, Umar A, Carethers JM, et al. Evidence for a connection between the mismatch repair system and the G(2) cell-cycle checkpoint. Cancer Res 1995;55:3721–5.
36. Alonso M, Hamelin R, Kim M, et al. Microsatellite instability occurs in distinct subtypes of pediatric but not adult central nervous system tumors. Cancer Res 2001;61:2124–8.
37. Martinez R, Schackert HK, Plaschke J, Baretton G, Appelt H, Schackert G. Molecular mechanisms associated with chromosomal and microsatellite instability in sporadic glioblastoma multiforme. Oncology 2004;66:395–403.

Downloaded from clincancerres.aacrjournals.org on September 30, 2020. © 2007 American Association for Cancer Research.

AACR American Association for Cancer Research

Clinical Cancer Research

Loss of the Mismatch Repair Protein MSH6 in Human Glioblastomas Is Associated with Tumor Progression during Temozolomide Treatment

Daniel P. Cahill, Kymberly K. Levine, Rebecca A. Betensky, et al.

Clin Cancer Res 2007;13:2038-2045.

Updated version	Access the most recent version of this article at: http://clincancerres.aacrjournals.org/content/13/7/2038
Supplementary Material	Access the most recent supplemental material at: http://clincancerres.aacrjournals.org/content/suppl/2007/04/03/13.7.2038.DC1

Cited articles	This article cites 37 articles, 17 of which you can access for free at: http://clincancerres.aacrjournals.org/content/13/7/2038.full#ref-list-1
Citing articles	This article has been cited by 39 HighWire-hosted articles. Access the articles at: http://clincancerres.aacrjournals.org/content/13/7/2038.full#related-urls

E-mail alerts	Sign up to receive free email-alerts related to this article or journal.
Reprints and Subscriptions	To order reprints of this article or to subscribe to the journal, contact the AACR Publications Department at pubs@aacr.org.
Permissions	To request permission to re-use all or part of this article, use this link http://clincancerres.aacrjournals.org/content/13/7/2038. Click on "Request Permissions" which will take you to the Copyright Clearance Center's (CCC) Rightslink site.

Downloaded from clincancerres.aacrjournals.org on September 30, 2020. © 2007 American Association for Cancer Research.